

**A point mutation in the extracellular domain of KIT promotes tumorigenesis of mast cells via ligand-independent auto-dimerization**

Yosuke Amagai<sup>1,2</sup>, Akira Matsuda<sup>3</sup>, Kyungsook Jung<sup>4,5</sup>, Kumiko Oida<sup>1</sup>, Hyosun Jang<sup>1</sup>, Saori Ishizaka<sup>1</sup>, Hiroshi Matsuda<sup>1,3\*</sup>, and Akane Tanaka<sup>1,4\*</sup>

<sup>1</sup>Cooperative Major in Advanced Health Science, Graduate School of Bio-Applications and System Engineering, Tokyo University of Agriculture and Technology, Tokyo, Japan

<sup>2</sup>Laboratory Animal Research Center, The Institute of Medical Science, The University of Tokyo, Tokyo, Japan

Laboratories of <sup>3</sup>Veterinary Molecular Pathology and Therapeutics and <sup>4</sup>Comparative Animal Medicine, Division of Animal Life Science, Institute of Agriculture, Tokyo University of Agriculture and Technology, Tokyo, Japan

<sup>5</sup>Eco-friendly Material Research Center, Korea Research Institute of Bioscience and Biotechnology, Jeonbuk, Korea

## Supplementary information

KIT model	Circle values
wild-type	2.43
D419del	3.95
D419del_R420W_L421G	2.64
Y418R_D419del_R420W	2.35
Y418A_D419del	2.44
T417I_Y418-D419del	3.59
D419-R420del_L421F	3.06
T417V_Y418-D419del	2.97
T417R_Y418G_D419del	4.23
T417N_Y418-D419del	3.19
Y418-D419insFF_R420G	5.27
A502-Y503insYA	3.91

**Table S1.** Circle values of mutant human KITs. Based on the algorithms of PDFAMS software, the circle values of mutant human KIT reported by Kohl *et al.*<sup>17</sup> and Lux *et al.*<sup>18</sup> were calculated. To compare the stability of all mutant KITs, circle values were calculated taking into consideration 24 amino acid residues (414–429, 449, 489–491, and 501–504), which are located within 4.0 Å from residues 417–421 or 501–504.

Figure S1

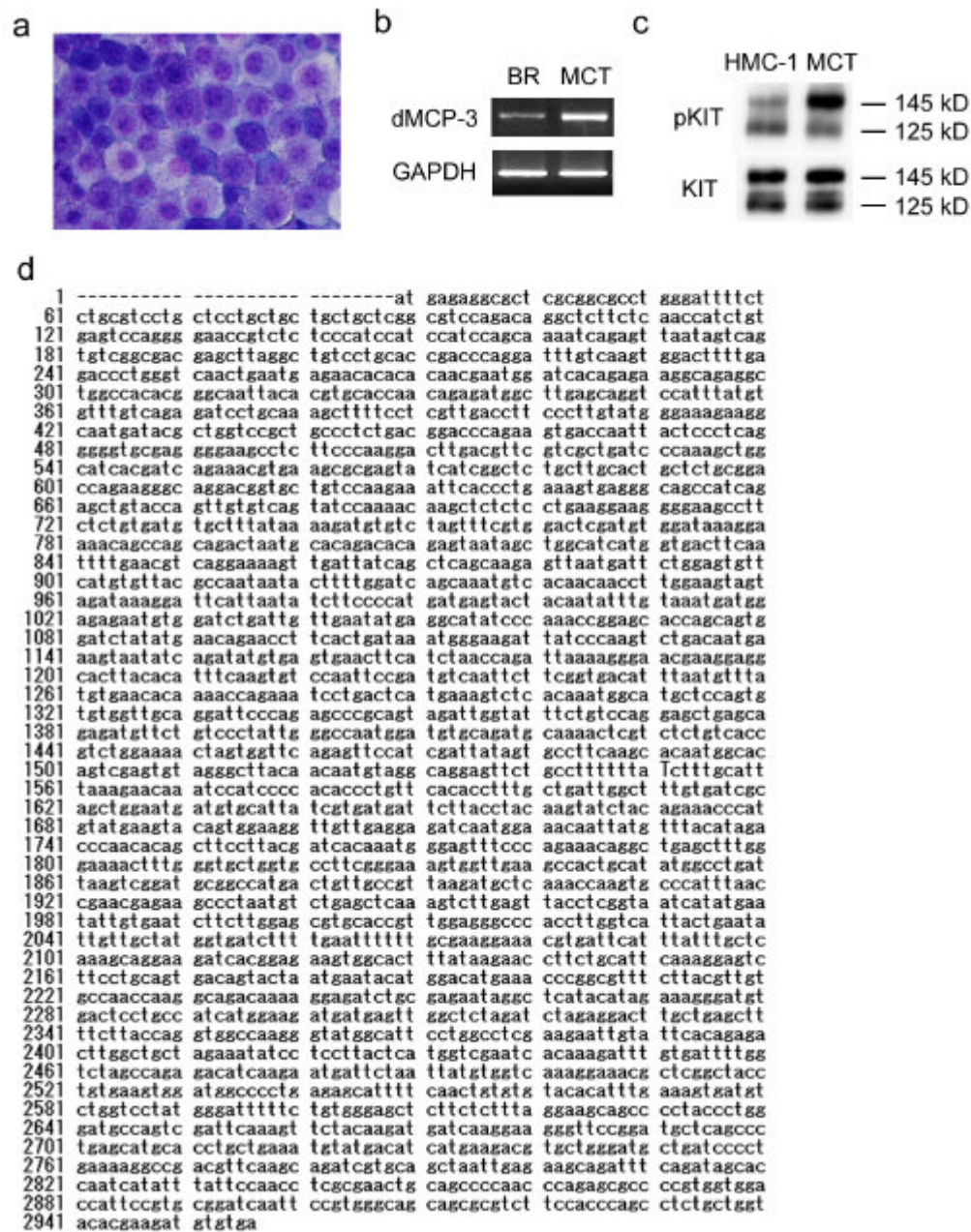
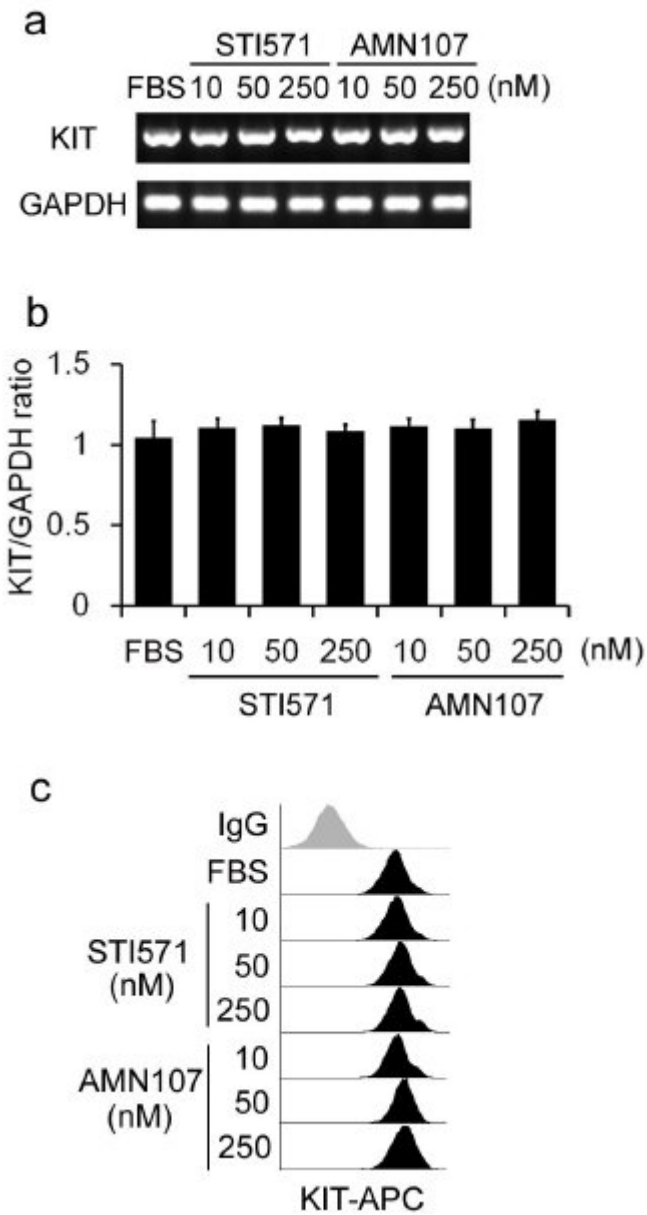


Figure S2



## Supporting figure legends

**Figure S1.** Characterization of a clinical MCT sample harboring the KIT Asn508Ile mutation.

(a) Cytospin preparation of primary cultured tumor cells. A dog was diagnosed with multiple grade II MCTs occurring in both the mammary gland and perianal region. Primary tumor cells were cultured in AIM-V medium following collagenase digestion. The image shows a cytospin preparation of the tumor obtained from the mammary gland, which was stained with toluidine blue. Original magnification,  $\times 200$ . (b) RT-PCR analysis of dMCP-3 expression in primary tumor cells. The data shown are representative of 2 independent experiments. The BR cell line is a tumor-derived canine mast cell line that was used as a positive control. (c) Western blot analysis of primary culture tumor cells. The phosphorylation status of KIT was examined using cell lysates of primary tumor cells grown in culture. HMC-1 cell lysates were used as a positive control. (d) The full length sequence of *c-kit* from a canine mast cell tumor with the 1551 A>T point mutation. Numbering corresponds to GenBank accession No. AF044249, and the capital “T” indicates the site of the 1551 A>T point mutation.

**Figure S2.** Effects of KIT inhibitors on *de novo* synthesis and internalization of KIT. (a)

Expression of KIT mRNA in IC-2<sup>N508I</sup> cells in the presence or absence of KIT inhibitors. RT-PCR analysis was performed using cells treated with the indicated concentrations of STI571 or AMN107 for 1 h. (b) The relative KIT/GAPDH expression ratios  $\pm$  SD from 3 independent experiments are indicated. (c) Cell surface expression of the KIT receptor in IC-2<sup>N508I</sup> cells in the presence or absence of KIT inhibitors. IC-2<sup>N508I</sup> cells were treated with STI571 or AMN107 for 4 h at the indicated concentrations, stained with an anti-KIT-APC antibody, and analyzed by flow cytometry analysis. Data shown are representative of 3 independent experiments.